Structure and superconductivity in compressed Li-Si-H compounds: Density functional theory calculations

Peiyu Zhang,[1,*] Ying Sun,[1,*] Xue Li,[1] Jian Lv,[1,†] and Hanyu Liu[1,2,‡]

[1]*International Center for Computational Method & Software, College of Physics, Jilin University, Changchun 130012, China*

[2]*State Key Laboratory of Superhard Materials and Key Laboratory of Physics and Technology for Advanced Batteries (Ministry of Education), College of Physics, and International Center of Future Science, Jilin University, Changchun 130012, China*

(Received 27 April 2020; revised 19 August 2020; accepted 20 October 2020; published 5 November 2020)

Previous experimental evidence showed that silane (SiH_4) becomes a superconductive phase at a critical temperature (T_c) of 17 K above 96 GPa, although this observation was not supported by later experiments due to the fact that SiH_4 was measured to decompose into amorphous silicon and solid hydrogen at ∼60–90 GPa and then recrystallized into a nonmetallic phase up to ∼130 GPa. Given lithium has a short atomic radius and low electronegativity, it could be incorporated into the binary hydrides and act as an electron donor by doping electrons into the lattice of parent binary hydrides, enabling the modification of crystal structures and superconductivity for the resulting ternary hydride system. In this work, therefore, we attempted to chemically tune crystal structures and improve the superconductivity of the Si-H system via lithium incorporation, by performing structure searching simulations on the Li-Si-H system at a wide pressure range of 50–350 GPa. As a result, four stable stoichiometries of $LiSiH_5$, $LiSiH_6$, $LiSi_2H_9$, and Li_2SiH_6, as well as two metastable stoichiometries of $LiSiH_4$ and $LiSiH_8$, were uncovered under high pressures. Among these predicted stoichiometries, $LiSi_2H_9$ and $LiSiH_8$ are predicted to become good phonon-mediated superconductors with estimated T_c of 54 and 77 K at 172 and 250 GPa, respectively. These results highlight the role of lithium incorporation in chemically tuning crystal structures, which induce the significant change of electronic properties for a Si-H system from nonmetallicity or poor metallicity to high-T_c superconductivity, shedding light on the exploration and discovery of high-T_c superconductivity in a variety of ternary hydrogen-rich compounds associated with lithium incorporation.

DOI: 10.1103/PhysRevB.102.184103

I. INTRODUCTION

Of particular interest is hunting high-temperature superconductors in compressed hydrogen-rich compounds due to the finding of a superconducting critical temperature (T_c) of 8 K in Th_4H_{15} at ambient pressure as early as in 1970 [1]. The idea for searching for high-T_c materials among hydrogen-rich compounds is not unreasonable since "chemical precompression" effects played a critical role in lowering the required pressure for the metallization of hydrogen-rich materials compared to pure solid hydrogen [2,3], as hydrogen is the lightest element and possibly gives rise to a high Debye temperature and a strong electron-phonon coupling necessary for a good phonon-mediated superconductor. Following this idea, much effort has been dedicated to the investigation of hydrogen-rich compounds under high pressure [4–10].

Recently, interest in hydrogen-rich compounds as a host candidate for high-temperature superconductors has received much more attention, due to the observations of compressed H-S [11] and La-H [12–14] systems with T_c above 200 K, as both are motivated and guided by the theoretical structure prediction [15–19], which opens an impetus to search for high-temperature superconductors in binary hydrides as well as ternary hydrides [4–10,20–24]. Recently, a metastable phase Li_2MgH_{16} [22] is predicted with a remarkably "hot" T_c above room temperature by gradually introducing the Li atom, which can act as a donor that dopes electrons into the lattice of MgH_{16} to effectively improve the superconductivity of the parent MgH_{16} system. Encouragingly, moreover, a very recent experimental work also reported a room-temperature superconductivity with a room T_c of 288 K in the C-S-H system at 267 GPa [25], indicating it seems to be a feasible way of searching for high-temperature superconductivity in ternary hydride systems.

This is reminiscent of SiH_4 having the highest hydrogen content among all binary hydrides at ambient conditions as being a promising candidate for a high-temperature superconductor at high pressure [2]. However, it remains an open question on the observation of the superconductivity in SiH_4 with a T_c of 17 K above 96 GPa [26–31]. Several theoretical studies suggested the superconductivity in the Si-H system at higher pressure [32–36]. It is noteworthy that our recent work indicates the low-electron-negativity Li may be helpful to tune the crystal structures and enhance the superconductivity for hydrogen-rich system by doping electrons into the lattice [24]. It is natural to wonder if this peculiar strategy could be considered to improve the superconductivity of the Si-H system via doping Li atoms into the lattice.

*These authors contributed equally to this work.
†lvjian@jlu.edu.cn
‡hanyuliu@jlu.edu.cn

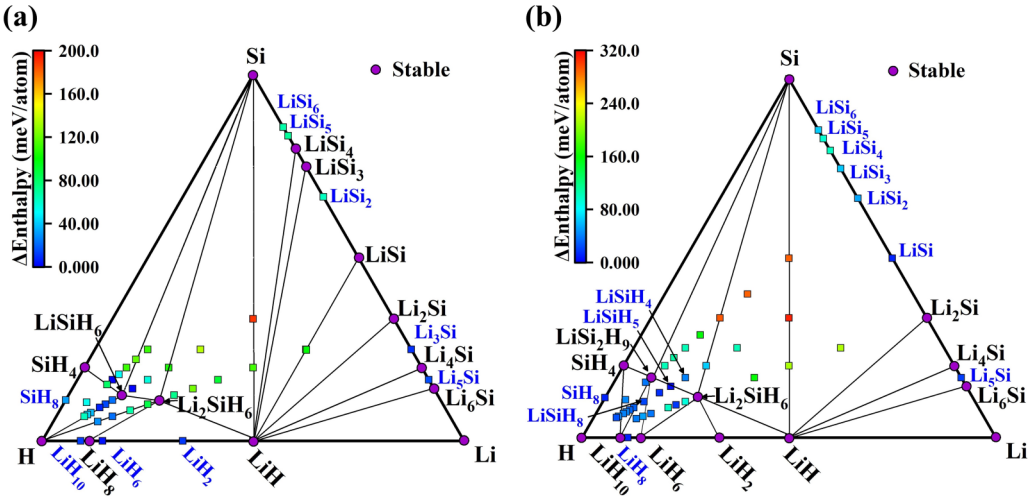

FIG. 1. Phase diagrams of $Li_xSi_yH_z$ relative to elemental Li [50], Si [51,52], H [53,54], binary Li-H [55,56], Li-Si [57], and Si-H [35,36,58] systems at (a) 100 and (b) 250 GPa by including zero-point energy. Purple solid circles and colored (relative metastability of $Li_xSi_yH_z$ above the convex hull in the unit of meV/atom) squares indicate stable and metastable phases, respectively. The structures of Li_xSi_y (x: 1–6, y: 1–6) at 250 GPa are predicted in this work, and structure parameters of energetically stable phases $I4/mmm$-Li_2Si, $Pnnm$-Li_4Si, and $C2/m$-Li_6Si are summarized in Table S1 in the Supplemental Material [59].

In this work, we have systematically explored the crystal structures and superconductivity of Li-Si-H ternary compounds at a pressure range of 50–350 GPa. As a result of extensive simulations, four stable stoichiometries of $LiSiH_5$, $LiSiH_6$, $LiSi_2H_9$, and Li_2SiH_6, as well as two metastable stoichiometries of $LiSiH_4$ and $LiSiH_8$, were uncovered through swarm-intelligence structure searching calculations (CALYPSO) [37–39]; this code has been benchmarked on various known systems with several successful structure predictions [40–43]. Furthermore, electron-phonon coupling calculations indicate that $P6_3/mmc$-$LiSiH_4$, P-3-$LiSi_2H_9$, and $C2/m$-$LiSiH_8$ are phonon-mediated superconductors with estimated T_c values of 40, 54, and 77 K with a typical μ^* of 0.1 at 200, 172, and 250 GPa, respectively. These simulations highlight the role of Li atoms in chemically tuning the structures and enhancing the superconductivity in a distinct class of ternary hydrides, thus opening an avenue to design high-T_c superconductors.

II. COMPUTATIONAL DETAILS

In order to investigate the stable structures in the Li-S-H system, we systematically employed a heuristic algorithm based on the particle swarm-intelligence approach as implemented in the CALYPSO code [37–39] for $Li_xSi_yH_z$ (x: 1–2; y: 1–2; z: 1–16) at the pressure range of 50–350 GPa, using simulation cells consisting of a maximal number of 38 atoms. The total number of predicted structures is at least ~200 000 in our structure searching simulations. For structural relaxations, we have performed the first-principles simulations using density functional theory (DFT) within the Perdew-Burke-Ernzerhof (PBE) parametrization of the generalized gradient approximation (GGA) [44], as implemented in the Vienna *Ab Initio* Simulation Package (VASP) code [45]. The all-electron projector-augmented wave (PAW) [46] method was adopted with $1s$, $1s^22s^1$, and $3s^23p^2$ considered as valence electrons for H, Li, and Si, respectively. A plane-wave energy cutoff of 650 eV was employed, and a Monkhorst-Pack Brillouin sampling grid of $2\pi \times 0.03$ Å^{-1} was selected. The electron-phonon coupling (EPC) simulations were well estimated by the QUANTUM ESPRESSO package [47]. GBRV ultrasoft pseudopotentials [48] for Li, Si, and H were employed, with kinetic energy cutoff and kinetic energy cutoff for charge density 60 and 480 Ry, respectively. A q mesh of $4 \times 4 \times 3$, $7 \times 7 \times 3$, and $3 \times 3 \times 6$, and a k mesh of $16 \times 16 \times 12$, $28 \times 28 \times 12$, and $12 \times 12 \times 24$, respectively, were used in the electron-phonon coupling calculations for P-3-$LiSi_2H_9$, $P6_3/mmc$-$LiSiH_4$, and $C2/m$-$LiSiH_8$. The threshold for self-consistency in the lattice dynamics was 1×10^{-12} Ry/cell. For calculating T_c of the predicted structure, previous studies suggest that a standard Allen-Dynes modified McMillan equation could be able to reasonably estimate T_c with the EPC parameter λ below 1.5 [49].

$$T_c = \frac{\omega_{\log}}{1.2} \exp\left[-\frac{1.04(1+\lambda)}{\lambda - \mu^*(1+0.62\lambda)}\right], \quad (1)$$

where parameters μ^* and $\omega_{\log}$ are the Coulomb pseudopotential and logarithmic average frequency, respectively, which could be numerically calculated by the QUANTUM ESPRESSO package.

III. RESULTS AND DISCUSSIONS

We have investigated the stability of the ternary Li-Si-H system by the calculation of formation enthalpies relative to elemental [50–54] and binary solids [35,36,55–58] of various Li-Si-H compounds, and constructed the ternary phase diagrams at 100 and 250 GPa with and without zero-point energy (ZPE) correction, as shown in Figs. 1 and S1 in the Supplemental Material [59]. Four stoichiometries of $LiSiH_5$, $LiSiH_6$, $LiSi_2H_9$, and Li_2SiH_6 become stable against decomposition into elemental or binary solids at several pressure points. Moreover, we found two additional hydrogen-rich stoichiometries, $LiSiH_4$ and $LiSiH_8$, with positive values of 41

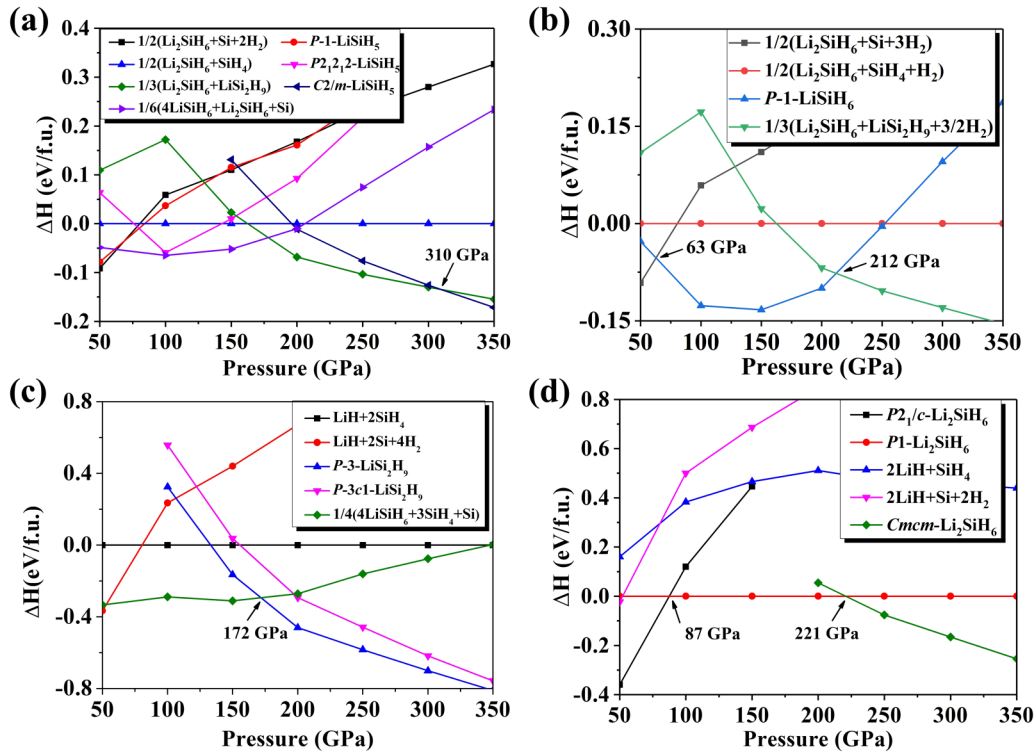

FIG. 2. Enthalpy curves per formula unit including zero-point energy as a function of pressure for (a) $LiSiH_5$ with respect to $Li_2SiH_6 + SiH_4$, (b) $LiSiH_6$ with respect to $Li_2SiH_6 + SiH_4 + H_2$, (c) $LiSi_2H_9$ with respect to $LiH + SiH_4$, and (d) Li_2SiH_6 with respect to $P1$-Li_2SiH_6.

and 22 meV/atom above the convex hull at 250 GPa. As shown in Figs. 1(b) and S1(b) [59], it is clearly seen that $LiSiH_5$ becomes thermodynamically unstable once ZPE correction is included, indicating there is a must to include ZPE correction for determining the stability of predicted structures in the ternary Li-Si-H system. Furthermore, we have systematically calculated the enthalpy difference of the four stable stoichiometries, as shown in Figs. 2, S(2), and S(3) [59]. Our simulations found that $LiSiH_5$ is stable with space group $C2/m$ above 310 GPa [Fig. 2(a)]. The other predicted phase P-1 is unstable with the ZPE correction effect. We found that $LiSiH_6$ is stable at a pressure range of 63–212 GPa with the symmetry space group P-1 [Fig. 2(b)]. For $LiSi_2H_9$, we found that it is stable against decomposition to LiH and SiH_4 at 172 GPa with the symmetry space group P-3, and a trigonal P-3c1 does not become energetically favorable until 350 GPa [Fig. 2(c)]. At 50 GPa, the monoclinic $P2_1/c$-Li_2SiH_6 is stable, and transforms into a $P1$ structure at 87 GPa, followed by a stable orthorhombic $Cmcm$ above 221 GPa [Fig. 2(d)].

For the metastable phases of $P6_3/mmc$-$LiSiH_4$ and $C2/m$-$LiSiH_8$, we propose three possible reaction routes to synthesize these predicted structures: (i) $SiH_4 + Li \rightarrow LiSiH_4$, (ii) $3/4SiH_4 + LiH + 1/4Si \rightarrow LiSiH_4$, and (iii) $SiH_4 + LiH + 3/2H_2 \rightarrow LiSiH_8$, with relative formation enthalpies at 250 GPa of −1.13, −0.01, and −0.04 eV/atom, respectively.

$C2/m$-$LiSiH_5$ [Fig. 3(a)] was found to contain SiH_{10} units, in which each Si atom connects ten H atoms with Si-H bonds ranging from 1.431 to 1.494 Å. For P-1-$LiSiH_6$ [Fig. 3(b)], each Si atom is bonded to seven H atoms forming edge-sharing SiH_7 octahedrons with the varied Si-H distances from 1.477 to 1.621 Å. We also found that there are H_2- molecule units in this structure with a bond length of 0.765 Å. For P-3-$LiSi_2H_9$ [Fig. 3(c)], each Si atom is surrounded by 12 H atoms, where Li atoms occupy interstitial positions in the lattice. SiH_6, SiH_9, and SiH_{10} units are found in $P2_1/c$-Li_2SiH_6 [Fig. 3(d)], $P1$-Li_2SiH_6 [Fig. 3(e)], and $Cmcm$-Li_2SiH_6 [Fig. 3(f)], respectively, with Si-H bond lengths of ∼1.409–1.609 Å. For $P6_3/mmc$-$LiSiH_4$ [Fig. 3(g)], each Si atom connected to the six nearest H atoms, and the SiH_8 units, are connected to form a thick layer in the ab plane with a Si-Si distance of 2.279 Å, and Li atoms also form a layered structure in the ab plane. For $C2/m$-$LiSiH_8$ [Fig. 3(h)], it consists of 11 coordinated Si atoms with the formation of shared SiH_{11} polyhedrons and H_2 units.

In order to investigate the dynamical stability of the candidate phases, we have performed the phonon simulations for all the predicted structures as shown in Fig. 4. The absence of any imaginary phonon frequency is found in the projected phonon density of states (PHDOS) of all the predicted structures, indicating that they are all dynamically stable. We also found PHDOS of Li and Si atoms occupied the lower-frequency region, since they both possess heavier mass compared to H atoms.

Furthermore, we have also carried out the simulations on the electronic properties of the predicted structures. The calculated projected electronic density of states (PDOS) indicated P-3-$LiSi_2H_9$, $P6_3/mmc$-$LiSiH_4$, and $C2/m$-$LiSiH_8$ are the metallic phase, as shown in Fig. 5, while the other stable phases show the nonmetallic feature. In addition, the PDOS near the Fermi energy level are mainly dominated by hydrogen atoms, indicating these phases may possess high

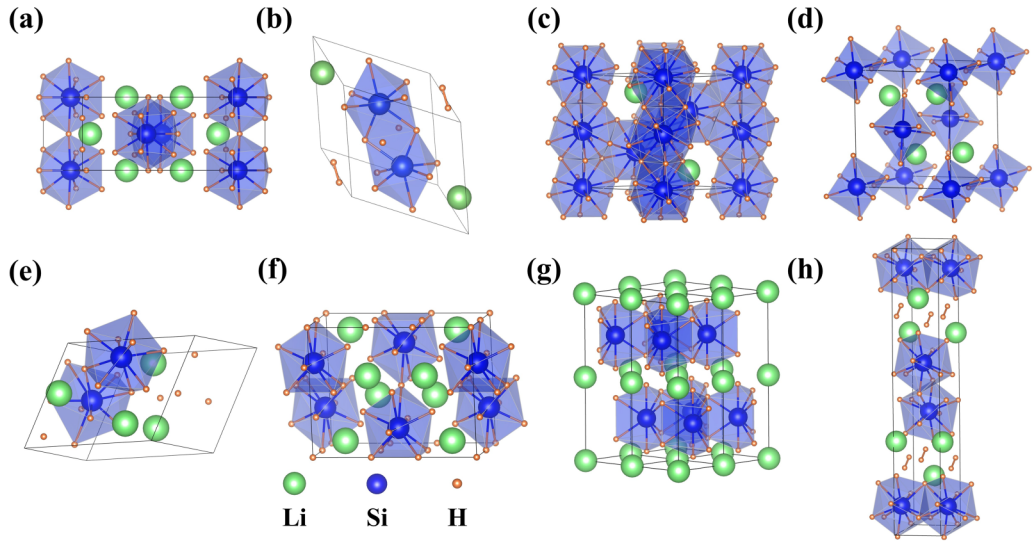

FIG. 3. Predicted crystal structures of (a) $C2/m$-$LiSiH_5$ at 350 GPa, (b) P-1-$LiSiH_6$ at 100 GPa, (c) P-3-$LiSi_2H_9$ at 150 GPa, (d) $P2_1/c$-Li_2SiH_6 at 50 GPa, (e) $P1$-Li_2SiH_6 at 100 GPa, (f) $Cmcm$-Li_2SiH_6 at 300 GPa, (g) $P6_3/mmc$-$LiSiH_4$ at 250 GPa, and (h) $C2/m$-$LiSiH_8$ at 250 GPa. More structure information of predicted structures is summarized in Table S2 in the Supplemental Material [59].

superconductivity as suggested in previous studies [10,18,24]. Moreover, $LiSi_2H_9$ is predicted to become thermodynamically stable down to 172 GPa, together with the calculated DOS, indicating this phase exhibits the metallic feature at a pressure range of 172–300 GPa. Our further Bader charge calculations [60] (Table S3 [59]) indicate the electrons transfer from Li and Si atoms to H atoms, where each Li atom loses ∼0.8e and each Si atom loses ∼3.0e, while H atoms accept electrons. However, we found that H atoms in P-1-$LiSiH_6$ (0.6e) and $C2/m$-$LiSiH_8$ (0.47e) accept fewer electrons than other phases. This is not unreasonable that both P-1-$LiSiH_6$ and $C2/m$-$LiSiH_8$ contain H_2-molecule units, which are unlikely to accept additional electrons by occupying antibonding orbitals of H_2 molecules. In order to identify the bonding feature in Li-Si-H compounds, we have calculated the electron localization functions (ELF) [61] for several predicted structures, as shown in Fig. S4 [59]. The results clearly show a typical ionic bonding feature between Li-H and Si-H, which is similar

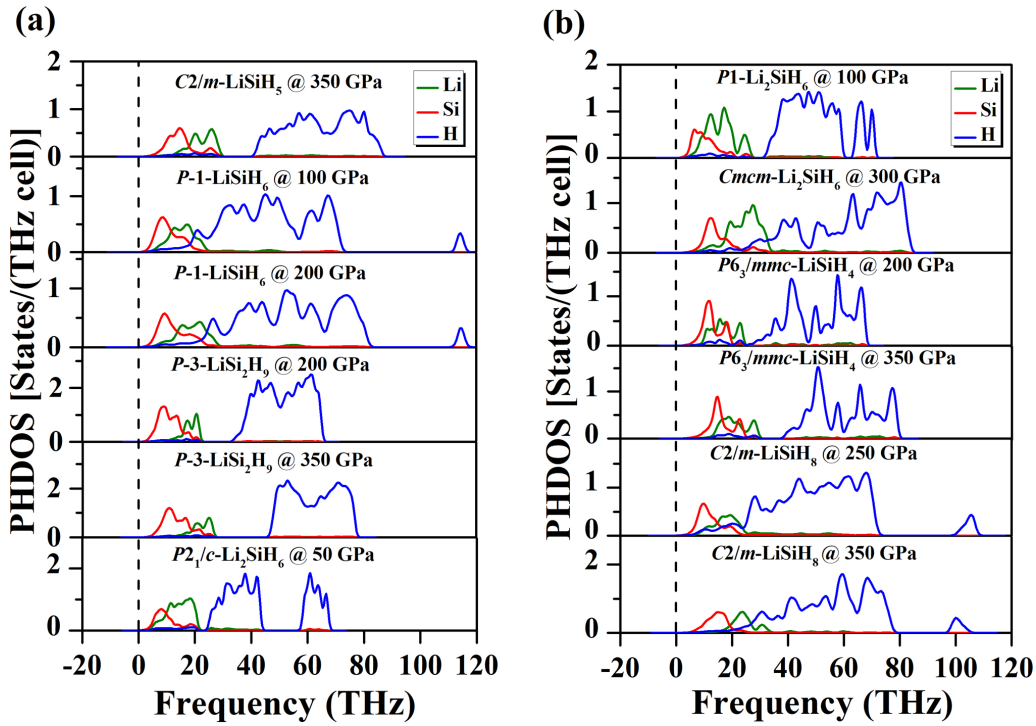

FIG. 4. The calculated PHDOS of predicted Li-Si-H compounds at high pressures.

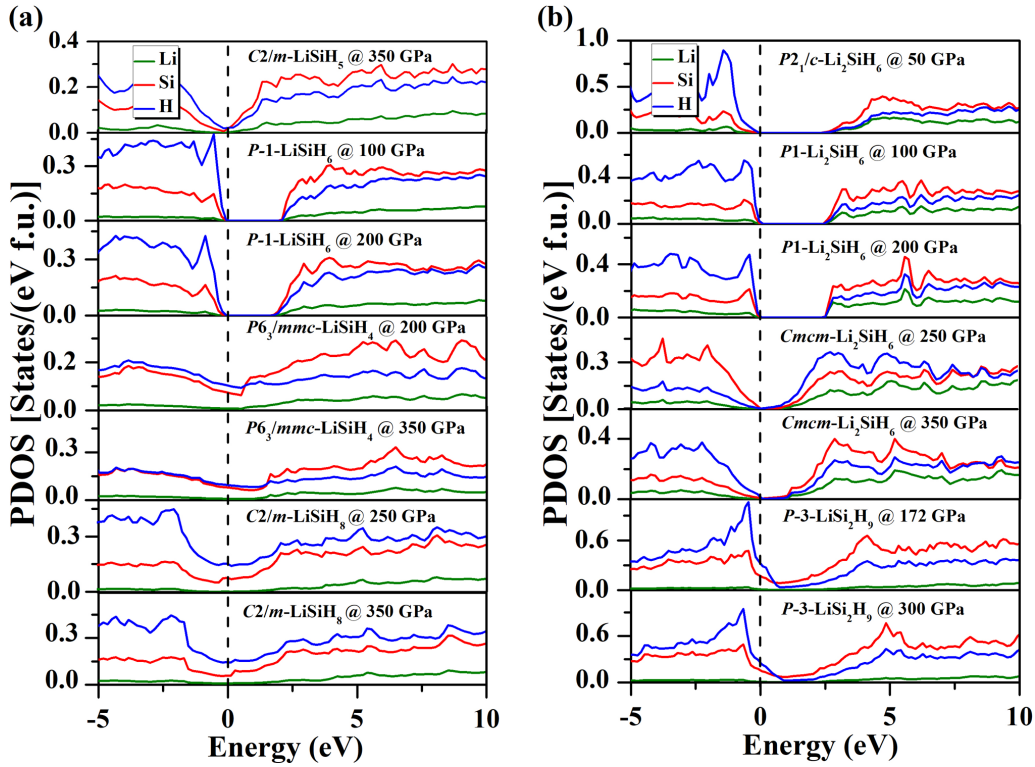

FIG. 5. The calculated PDOS of various Li-Si-H compounds at high pressures. The vertical dashed lines indicate Fermi energy level.

to the bonding feature between metal elements and hydrogen in the Mg-Si-H [62] and Mg-Ge-H [63] systems.

Motivated by the appearance of large values of hydrogen-derived electronic DOS at the Fermi energy level for predicted P-3-$LiSi_2H_9$, $P6_3/mmc$-$LiSiH_4$, and $C2/m$-$LiSiH_8$, we subsequently explored the superconductivity of these structures at different pressures through the Allen-Dynes modified McMillan equation [49], as shown in Table I. As a result, the obtained EPC parameter λ is 0.77 and the logarithmic average phonon frequency $\omega_{\log}$ is 1251 K for P-3-$LiSi_2H_9$ at 172 GPa, which leads to an estimated T_c of 43–54 K with a typical value of $\mu^* = 0.1$–0.13. $LiSiH_8$ has the highest hydrogen content among all predicted structures; a high T_c of this phase is thus expected. Furthermore, we explored the superconductivity of $LiSiH_8$, and the results indicate that this phase indeed has a moderate value λ of 1.08, together with $\omega_{\log}$ of 989 K, leading to a high T_c of 77 K with $\mu^* = 0.1$ at 250 GPa. In addition, we found that T_c values are depressed with increasing pressure for all predicted structures, where lower values of N_{Ef} and λ were identified upon compression.

IV. CONCLUSIONS

In summary, we have explored the crystal structures and superconductivity of Li-Si-H ternary compounds at a pressure range of 50–350 GPa, by using structure searching simulations within the framework of density functional theory. As a result of extensive structure searching simulations, four stable stoichiometries of $LiSiH_5$, $LiSiH_6$, $LiSi_2H_9$, and Li_2SiH_6, as well as two metastable stoichiometries of $LiSiH_4$ and $LiSiH_8$, were uncovered at high pressures. Bader charge simulations and ELF calculations reveal the ionic feature of Li-H and Si-H bonds. Further EPC simulations indicate predicted $LiSi_2H_9$, $LiSiH_4$, and $LiSiH_8$ are superconductive

TABLE I. Superconducting parameters of the metallic Li-Si-H phases.

Compound	Space group	Pressure (GPa)	λ	$\omega_{\log}$ (K)	N_{Ef} (States/Ry/f.u.)	T_c(K) $\mu^* = 0.1$	T_c(K) $\mu^* = 0.13$
$LiSi_2H_9$	P-3	172	0.77	1251	10.52	54	43
		200	0.69	1318	9.71	44	34
		300	0.51	1464	7.35	19	12
$LiSiH_4$	$P6_3/mmc$	200	0.64	1424	3.99	40	29
		300	0.49	1717	3.55	20	12
		350	0.46	1827	3.42	15	8
$LiSiH_8$	$C2/m$	250	1.08	989	4.59	77	67
		300	0.91	1226	4.33	73	62
		350	0.84	1315	4.10	68	56

phases with estimated T_cs of 43–54, 29–40, 67–77 K at 172, 200, and 250 GPa, respectively, using μ^* of 0.1–0.13. Our current results highlight the effective chemical tuning of the stabilized structures and the enhanced superconductivity in a distinct class of ternary hydrides, offering insights for further designing and optimizing high-T_c superconductors.

ACKNOWLEDGMENTS

This work is supported by the National Natural Science Foundation of China (Grants No. 11534003, No. 11874175, No. 11874176, and No. 12074138), Science Challenge Project No. TZ2016001, the Fundamental Research Funds for the Central Universities (Jilin University, JLU), the Program for JLU Science and Technology Innovative Research Team (JLUSTIRT), the Strategic Priority Research Program of Chinese Academy of Sciences (Grant No. XDB33000000), and National Key Research and Development Program of China (under Grant No. 2016YFB0201201). The authors also acknowledge the funding support from Jilin Province Outstanding Young Talents project (Grant No. 20190103040JH). We used the computing facilities at the High-Performance Computing Centre of Jilin University and Tianhe2-JK at the Beijing Computational Science Research Centre.

[1] C. Satterthwaite and I. Toepke, Phys. Rev. Lett. **25**, 741 (1970).
[2] N. W. Ashcroft, Phys. Rev. Lett. **92**, 187002 (2004).
[3] J. J. Gilman, Phys. Rev. Lett. **26**, 546 (1971).
[4] C. J. Pickard, I. Errea, and M. I. Eremets, Annu. Rev. Condens. Matter Phys. **11**, 57 (2020).
[5] J. A. Flores-Livas, L. Boeri, A. Sanna, G. Profeta, R. Arita, and M. Eremets, Phys. Rep. **856**, 1 (2020).
[6] A. R. Oganov, C. J. Pickard, Q. Zhu, and R. J. Needs, Nat. Rev. Mater. **4**, 331 (2019).
[7] E. Zurek and T. Bi, J. Chem. Phys. **150**, 050901 (2019).
[8] T. Bi, N. Zarifi, T. Terpstra, and E. Zurek, in *Reference Module in Chemistry, Molecular Sciences and Chemical Engineering* (Elsevier, Amsterdam, 2019), https://doi.org/10.1016/B978-0-12-409547-2.11435-0.
[9] H. Wang, X. Li, G. Gao, Y. Li, and Y. Ma, WIREs Comput. Mol. Sci. **8**, e1330 (2018).
[10] L. Zhang, Y. Wang, J. Lv, and Y. Ma, Nat. Rev. Mater. **2**, 17005 (2017).
[11] A. Drozdov, M. Eremets, I. Troyan, V. Ksenofontov, and S. Shylin, Nature **525**, 73 (2015).
[12] Z. M. Geballe, H. Liu, A. K. Mishra, M. Ahart, M. Somayazulu, Y. Meng, M. Baldini, and R. J. Hemley, Angew. Chem. **57**, 688 (2018).
[13] A. P. Drozdov, P. P. Kong, V. S. Minkov, S. P. Besedin, M. A. Kuzovnikov, S. Mozaffari, L. Balicas, F. F. Balakirev, D. E. Graf, V. B. Prakapenka, E. Greenberg *et al.*, Nature **569**, 528 (2019).
[14] M. Somayazulu, M. Ahart, A. K. Mishra, Z. M. Geballe, M. Baldini, Y. Meng, V. V. Struzhkin, and R. J. Hemley, Phys. Rev. Lett. **122**, 027001 (2019).
[15] Y. Li, J. Hao, H. Liu, Y. Li, and Y. Ma, J. Chem. Phys. **140**, 174712 (2014).
[16] D. Duan, Y. Liu, F. Tian, D. Li, X. Huang, Z. Zhao, H. Yu, B. Liu, W. Tian, and T. Cui, Sci. Rep. **4**, 6968 (2014).
[17] H. Liu, I. I. Naumov, R. Hoffmann, N. Ashcroft, and R. J. Hemley, Proc. Natl. Acad. Sci. USA **114**, 6990 (2017).
[18] F. Peng, Y. Sun, C. J. Pickard, R. J. Needs, Q. Wu, and Y. Ma, Phys. Rev. Lett. **119**, 107001 (2017).
[19] H. Liu, I. I. Naumov, Z. M. Geballe, M. Somayazulu, J. S. Tse, and R. J. Hemley, Phys. Rev. B **98**, 100102(R) (2018).
[20] J. Ying, X. Li, E. Greenberg, V. B. Prakapenka, H. Liu, and V. V. Struzhkin, Phys. Rev. B **99**, 224504 (2019).
[21] H. Li, X. Li, H. Wang, G. Liu, Y. Li, and H. Liu, New J. Phys. **21**, 123009 (2019).
[22] Y. Sun, J. Lv, Y. Xie, H. Liu, and Y. Ma, Phys. Rev. Lett. **123**, 097001 (2019).
[23] H. Li, Y. Sun, G. Liu, H. Wang, and H. Liu, Solid State Commun. **309**, 113820 (2020).
[24] X. Li, Y. Xie, Y. Sun, P. Huang, H. Liu, C. Chen, and Y. Ma, J. Phys. Chem. Lett. **11**, 935 (2020).
[25] E. Snider, N. Dasenbrock-Gammon, R. McBride, M. Debessai, H. Vindana, K. Vencatasamy, K. V. Lawler, A. Salamat, and R. P. Dias, Nature **586**, 373 (2020).
[26] M. Eremets, I. Trojan, S. Medvedev, J. Tse, and Y. Yao, Science **319**, 1506 (2008).
[27] O. Degtyareva, J. E. Proctor, C. L. Guillaume, E. Gregoryanz, and M. Hanfland, Solid State Commun. **149**, 1583 (2009).
[28] M. Hanfland, J. E. Proctor, C. L. Guillaume, O. Degtyareva, and E. Gregoryanz, Phys. Rev. Lett. **106**, 095503 (2011).
[29] T. A. Strobel, A. F. Goncharov, C. T. Seagle, Z. Liu, M. Somayazulu, V. V. Struzhkin, and R. J. Hemley, Phys. Rev. B **83**, 144102 (2011).
[30] T. Scheler, O. Degtyareva, M. Marqués, C. L. Guillaume, J. E. Proctor, S. Evans, and E. Gregoryanz, Phys. Rev. B **83**, 214106 (2011).
[31] G. Liu, Z. Yu, S. Li, and H. Wang, Mater. Lett. **249**, 84 (2019).
[32] J. Feng, W. Grochala, T. Jaron, R. Hoffmann, A. Bergara, and N. W. Ashcroft, Phys. Rev. Lett. **96**, 017006 (2006).
[33] Y. Yao, J. Tse, Y. Ma, and K. Tanaka, Europhys. Lett. **78**, 37003 (2007).
[34] X. J. Chen, J. L. Wang, V. V. Struzhkin, H. K. Mao, R. J. Hemley, and H. Q. Lin, Phys. Rev. Lett. **101**, 077002 (2008).
[35] M. Martinez-Canales, A. R. Oganov, Y. Ma, Y. Yan, A. O. Lyakhov, and A. Bergara, Phys. Rev. Lett. **102**, 087005 (2009).
[36] W. Cui, J. Shi, H. Liu, Y. Yao, H. Wang, T. Iitaka, and Y. Ma, Sci. Rep. **5**, 13039 (2015).
[37] Y. Wang, J. Lv, L. Zhu, and Y. Ma, Phys. Rev. B **82**, 094116 (2010).
[38] Y. Wang, J. Lv, L. Zhu, and Y. Ma, Comput. Phys. Commun. **183**, 2063 (2012).
[39] B. Gao, P. Gao, S. Lu, J. Lv, Y. Wang, and Y. Ma, Sci. Bull. **64**, 301 (2019).
[40] J. Zhang, J. Lv, H. Li, X. Feng, C. Lu, S. A. T. Redfern, H. Liu, C. Chen, and Y. Ma, Phys. Rev. Lett. **121**, 255703 (2018).
[41] P. Huang, H. Liu, J. Lv, Q. Li, C. Long, Y. Wang, C. Chen, R. J. Hemley, and Y. Ma, Proc. Natl. Acad. Sci. USA **117**, 5638 (2020).

[42] X. Zhong, M. Xu, L. Yang, X. Qu, L. Yang, M. Zhang, H. Liu, and Y. Ma, npj Comput. Mater. **4**, 1 (2018).
[43] L. Zhu, G. M. Borstad, H. Liu, P. A. Guńka, M. Guerette, J. Dolyniuk, Y. Meng, E. Greenberg, V. B. Prakapenka, B. L. Chaloux, A. Epshteyn *et al.*, Sci. Adv. **6**, eaay8361 (2020).
[44] J. P. Perdew, K. Burke, and M. Ernzerhof, Phys. Rev. Lett. **77**, 3865 (1996).
[45] G. Kresse and J. Furthmüller, Phys. Rev. B **54**, 11169 (1996).
[46] P. E. Blöchl, Phys. Rev. B **50**, 17953 (1994).
[47] P. Giannozzi, S. Baroni, N. Bonini, M. Calandra, R. Car, C. Cavazzoni, D. Ceresoli, G. L. Chiarotti, M. Cococcioni, I. Dabo, A. D. Corso *et al.*, J. Phys.: Condens. Matter **21**, 395502 (2009).
[48] K. F. Garrity, J. W. Bennett, K. M. Rabe, and D. Vanderbilt, Comput. Mater. Sci. **81**, 446 (2014).
[49] P. B. Allen and R. Dynes, Phys. Rev. B **12**, 905 (1975).
[50] J. Lv, Y. Wang, L. Zhu, and Y. Ma, Phys. Rev. Lett. **106**, 015503 (2011).
[51] H. Olijnyk, S. Sikka, and W. Holzapfel, Phys. Lett. A **103**, 137 (1984).
[52] S. J. Duclos, Y. K. Vohra, and A. L. Ruoff, Phys. Rev. Lett. **58**, 775 (1987).
[53] C. J. Pickard and R. J. Needs, Nat. Phys. **3**, 473 (2007).
[54] H. Liu, H. Wang, and Y. Ma, J. Phys. Chem. C **116**, 9221 (2012).
[55] E. Zurek, R. Hoffmann, N. Ashcroft, A. R. Oganov, and A. O. Lyakhov, Proc. Natl. Acad. Sci. USA **106**, 17640 (2009).
[56] Y. Chen, H. Y. Geng, X. Yan, Y. Sun, Q. Wu, and X. Chen, Inorg. Chem. **56**, 3867 (2017).
[57] S. Zhang, Y. Wang, G. Yang, and Y. Ma, ACS Appl. Mater. Inter. **8**, 16761 (2016).
[58] Y. Li, G. Gao, Y. Xie, Y. Ma, T. Cui, and G. Zou, Proc. Natl. Acad. Sci. USA **107**, 15708 (2010).
[59] See Supplemental Material at http://link.aps.org/supplemental/10.1103/PhysRevB.102.184103 for structure information and physical properties of $Li_xSi_yH_z$.
[60] R. F. Bader, Acc. Chem. Res. **18**, 9 (1985).
[61] A. D. Becke and K. E. Edgecombe, J. Chem. Phys. **92**, 5397 (1990).
[62] Y. Ma, D. Duan, Z. Shao, H. Yu, H. Liu, F. Tian, X. Huang, D. Li, B. Liu, and T. Cui, Phys. Rev. B **96**, 144518 (2017).
[63] Y. Ma, D. Duan, Z. Shao, D. Li, L. Wang, H. Yu, F. Tian, H. Xie, B. Liu, and T. Cui, Phys. Chem. Chem. Phys. **19**, 27406 (2017).